RÍO PAPALOAPAN BRIDGE: DESIGN AND SUCCESSFUL APPLICATION OF SPECIAL NON DESTRUCTIVE INSPECTION TECHNIQUES

J. A. López-López, J. A. Quintana-Rodríguez, F. J. Carrión-Viramontes, José Luis Moreno-Jiménez
Instituto Mexicano del Transporte, Carretera Querétaro-Galindo Km. 12, 76703, Sanfandila, Pedro Escobedo, Querétaro, México.
jalopez@imt.mx, alfredo_lopez@yahoo.com

ABSTRACT

This work describes the Non Destructive Tests (NDT) that were developed and applied in the *Río Papalopan* Bridge to analyze and to evaluate the structural condition of the upper anchorage elements of the bridge's cables. This project initiated from the failure of one of them in 2000; since then, a series of studies were generated to investigate this problem and for the rehabilitation of the bridge.

As a result of the failure analysis done in 2000, it was found that microstructural defects in the steel of the anchorage element were the main cause, mostly because of deficiencies in the manufacture process. Because of that, a NDT method was developed to identify anchorage elements in service with similar characteristics to the failed one. In 2003, the ultrasonic inspection technique was used to detect the microstructural defects and 16 elements were found as probable to fail, so it was proposed to change. In 2008, the rehabilitation of the bridge considered the change of 20 elements (4 in good condition for a reliability study). During the rehabilitation process, 3 different NDT were used: ultrasonic, liquid penetrant, and vibrations. The first two, to detect cracks in the welded unions, and the third, to calculate the load distribution in the cables at each rehabilitation stage.

Keywords: Non Destructive Tests, Fracture, Cable Stayed Bridge

1. INTRODUCTION

In 2000, a series of studies were initiated to investigate the main cause of failure of the upper anchorage element of one cable, in the Rio Papaloapan Stayed Bridge; where it was found that microstructural defects in the steel of the anchorage element (due to a deficient manufacturing process), were the key reason for the collapse of the cable. Once the source of the problem was identified, studies continued to find out the best rehabilitation strategy for the bridge, taking into consideration that the remaining anchorage element could have similar structural deficiencies with a high probability of failure.

The first challenge was to identify similar microstructural defects in the 111 anchorage elements in service (partially embedded in concrete), as compared to the failed one. For that reason, a non destructive inspection method was developed based on an ultrasonic technique, and after inspection in 2003, 16 upper anchorage elements were recognized as probable to fail and replacement was recommended. In 2008, the rehabilitation of the bridge considered the change of 20 upper anchorage elements (4 in good condition for a reliability study) [1].

1.1. Description of the Río Papaloapan Bridge

The Río Papaloapan Bridge is a cable-stayed structure with a main span of 203 m and a total length of 343 m, located in the State of Veracruz in Mexico. The bridge has 112 cables distributed in 8 semi-harps with 14 cables each. For identification reasons, the semi-harps were identified from 1 to 8 as indicated in Fig. 1 and 2, and cables were labeled from 1 to 14, starting with the shortest to the longest.

Figure1 – General view of the Rio Papaloapan Bridge

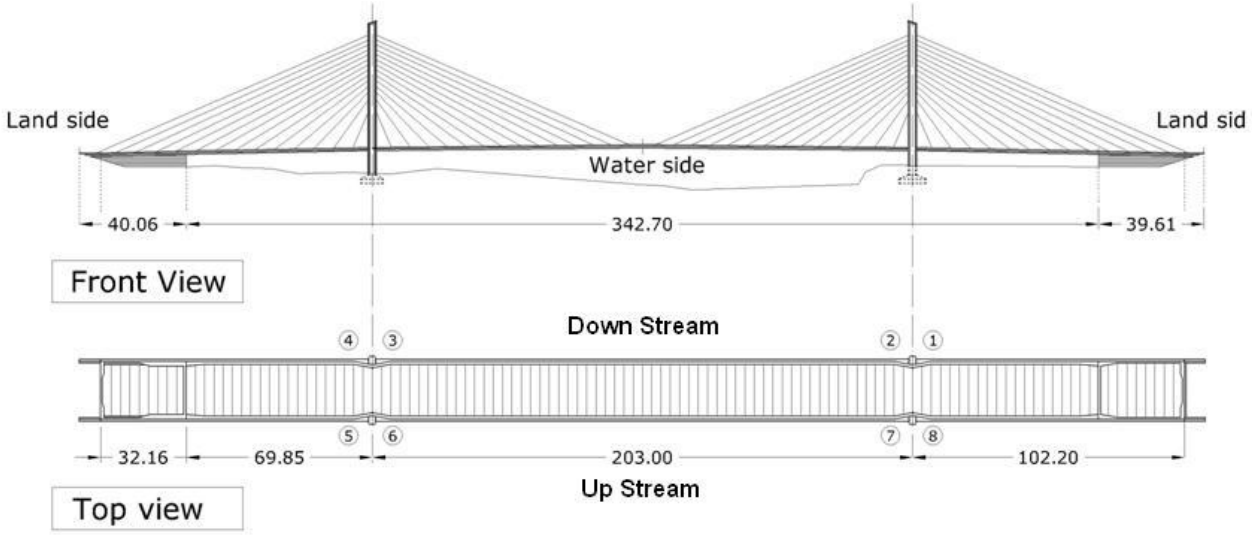

Figure 2 - Front and top view diagrams of the bridge

The unique design for the upper anchorage system of the cables was developed by Astiz [2] and consists of a steel tapered plate welded to the anchorage element, which is cylindrical shaped on one side to link to the cable cap, and flat on the other side to link to the tapered plate (Fig. 3).

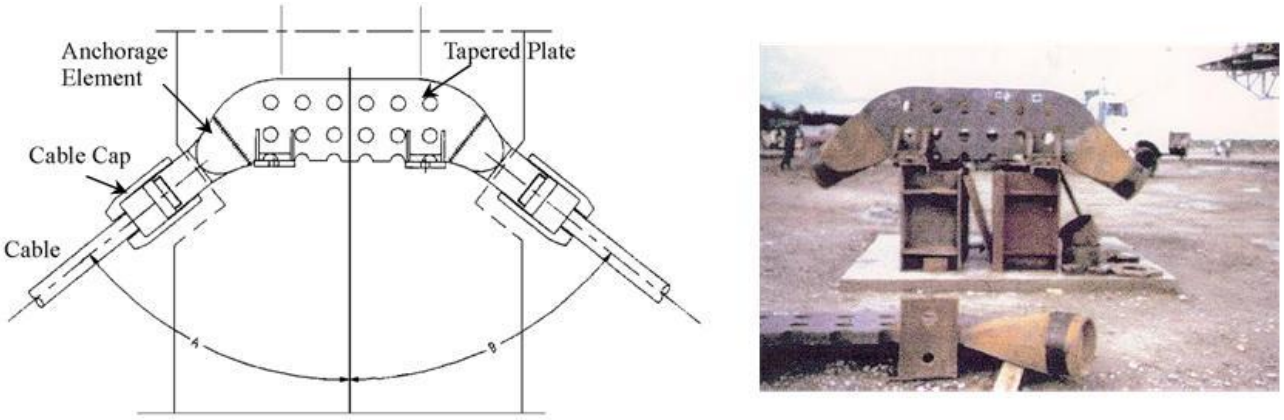

(a) Assembly design (b) Assembly before installation

Figure 3 - Upper anchorage assembly used for the cable system of the Río Papaloapan Bridge

1.2. Failure Analysis

In January 2000, the failure of the upper anchorage element from cable 11, semi-harp 7 (Fig. 4), lead to a series of analysis, concluding that its constitutive material was structurally deficient [3,4].

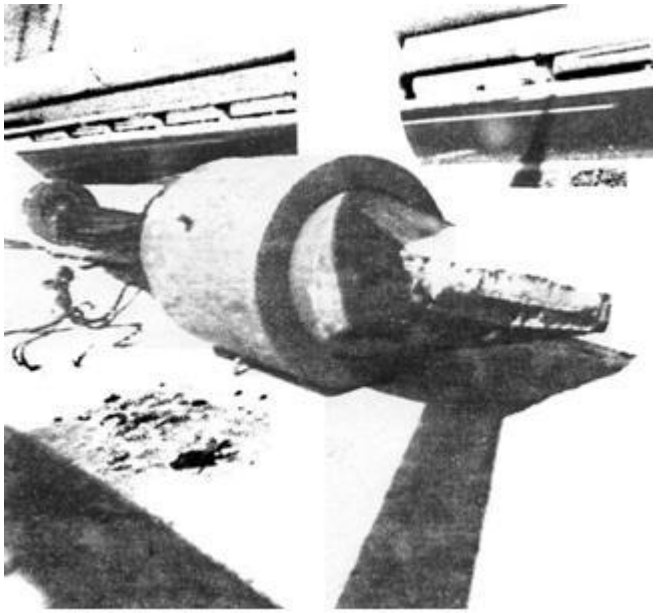

Figure 4 - Failed upper anchorage element from cable 11, semi-harp 7, occurred on January 2000 [3].

While the fracture took place close to the heat affected zone (HAZ), two initial hypotheses were focused on the steel quality of the upper anchorage element and on the heat treatment process given after welding. Later results showed that, although the chemical content of the material, and the yield and ultimate strengths were all within design specification of ASTM A148-80/50 steel [5], three main problems were identified [4]. As the piece was manufactured from a cast process; first, it had a high content of pores (Fig. 5); second, the steel was not properly normalized with a large grain size microstructure (ASTM 2) as it can be seen in Fig. 6; and third, elongation was 3%, far below to the 22% specification.

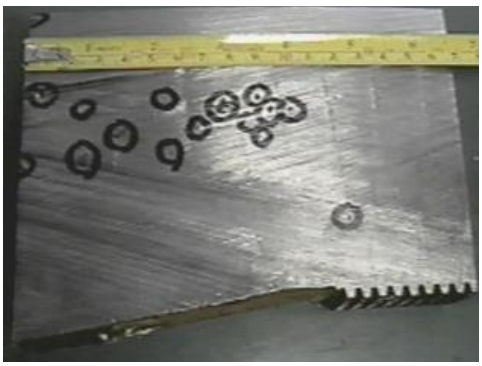

Figure 5 - Section of the upper anchorage element with high content of pores

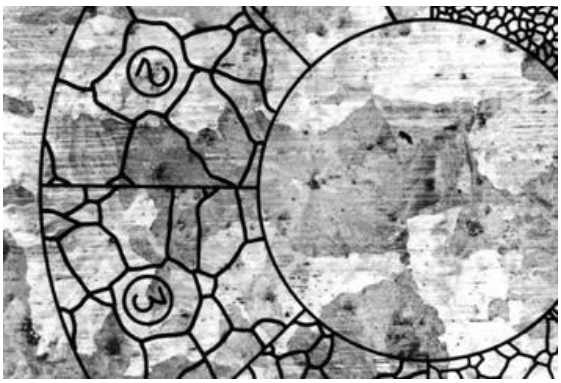

Figure 6 - Picture of the upper anchorage steel microstructure

To complete the analysis, fatigue crack propagation tests were performed to estimate fracture toughness and the coefficients according to Paris model [6]. Three point bending specimens were used according to ASTM E399 standard dimensions [7] with a specimen width of 16 mm and an initial crack length of 5.2 mm; tests were executed according to ASTM E647 standard [8] and a force ratio of 0.1.

Fig. 7 shows a typical fatigue plot for ΔK to da/dn, from the crack propagation test and with the data fitted to Paris model [6]; calculations from the experimental tests, the fracture toughness and the coefficients for the Paris equation model for the anchorage steel are presented in Table 1. It should be mentioned that typical values of steels for the exponent in Paris equation (m) fall between 2 and 4; that is, a value of 10.9 corresponds to steel with a high fracture growth rate, compared to typical values.

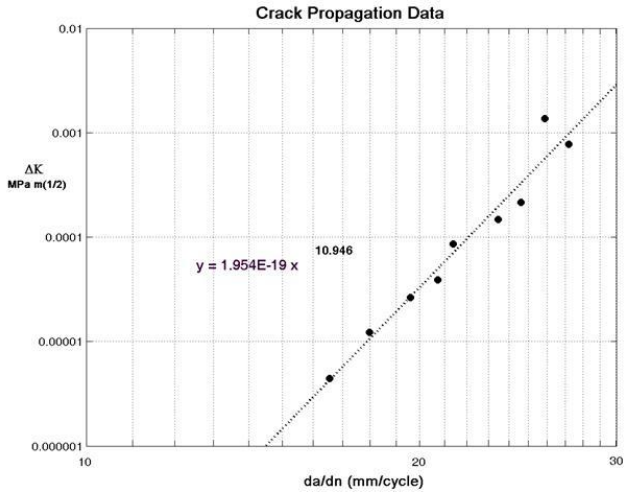

Figure 7 - Results from the crack propagation test (ΔK vs. da/dn), according to Paris model [6]

Table 1 - Paris coefficients and fracture toughness

Mechanical property		**Experimental Value**
Coefficients to Paris Model Equation	M	10.9
	C	1.9×10^{-19}
Fracture Toughness	K_{IC} [MPa $\sqrt{m}$]	26

2. ULTRASONIC INSPECTION FOR STRUCTURAL QUALIFICATION IN 2003

As it was mentioned, the need for the study was recognized after the identification of microstructural deficiencies in the anchorage element that failed in 2000, where large grain sizes (ASTM 2) and high pore content were the two main problems classified as critical due to brittleness and stress concentrations, resulting in low fracture toughness and high fatigue crack growth rate. While the main concern was focused on the 111 remaining anchorage elements, it was decided to use the ultrasonic inspection to evaluate the microstructure of those remaining elements. The basic approach was based on the analysis of the back wall reflections of a straight ultrasonic beam, which is highly dependent on the material's grain size [9]. To calibrate the inspection method, a reference block, with the same steel from the anchorage, was manufactured with two different grain sizes, ASTM 1 and 2 and 7 and 8 (Fig. 8). A comparison of the reflections from the reference block for both grain sizes is shown in Fig. 9, where energy dissipation in large grain size is significantly different from the one in small grain size.

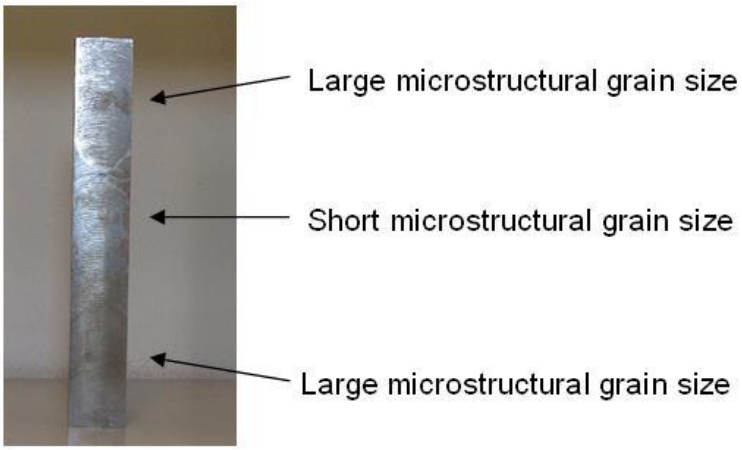

Figure 8 - Reference block for ultrasonic test.

Since the anchorage elements are almost completely embedded in concrete, field inspections were limited to the accessibility of the exposed surface (Fig. 10). Therefore, the inspections were complemented with 45 degree angle beam techniques to examine the internal zones of the element up to the welded zone to detect flaws in the material (Fig. 11).

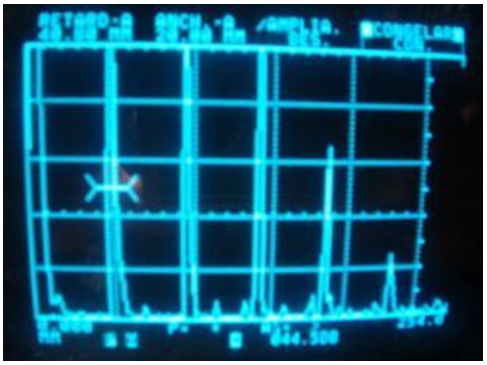

(a) Back wall reflections from the ASTM 7 and 8 grain size

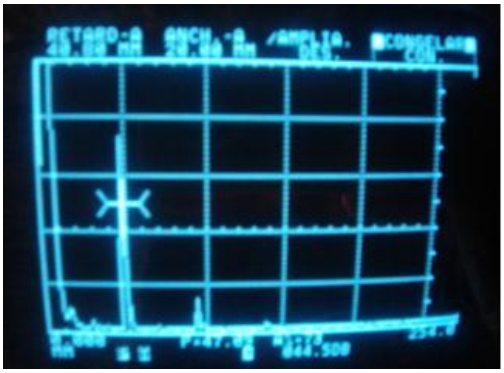

(b) Back wall reflections from the ASTM 1 and 2 grain size

Figure 9 - Comparison of the back wall reflections of the two different grain sizes in the reference block

Figure 10 - Accessibility for the ultrasonic inspection of a cable upper anchorage element

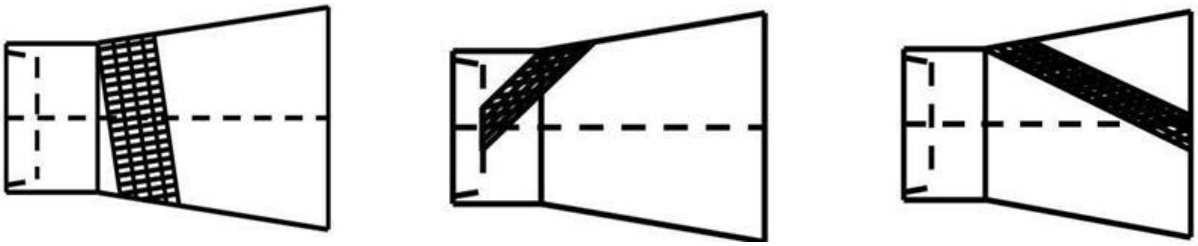

(a) Straight UT beam

(b) 45° angle beam to internal zone

(c) 45° angle beam to welded zone

Figure 11 - Regions inspected with the straight and angle beam ultrasonic techniques

The identified microstructural deficiencies from the ultrasonic inspection of the upper anchorage elements were classified as large grain size, probable large grain size, and high pore content [1]. Probable large grain size was defined for relative high energy dissipation, but less than the observed for ASTM 2. Table 2 shows a summary of the ultrasonic results. It must be pointed out that the bridge has 3 different designs for the upper anchorage elements: 26 elements type 1, 62 elements type 2, and 24 elements type 3; all the large grain size and probable large grain size elements were type 2, and the high pore content was found in one type 1 element and another type 3 element.

Table 2 - Summary results from field UT in the Río Papaloapan Bridge

Structural deficiency	**Number of anchorage elements**	**Type of element**
Large Grain Size (ASTM 2)	8	2
High Pore Content	2	1 and 3
Probable large Grain Size	6	2

Once the structural deficient elements were identified, a rehabilitation project was proposed to replace these elements and an integrity analysis was required to evaluate the structural reliability of the remaining elements, considering the statistical characterization of their microstructural, mechanical and chemical properties. While the characterization from the 16 deficient elements was not sufficient, 4 elements classified as in good condition were included in the rehabilitation project to obtain the complementary data necessary to characterize statistically all the elements (Fig.12). For the good condition elements, 1 was type 1, 2 were type 2 and 1 was type 3.

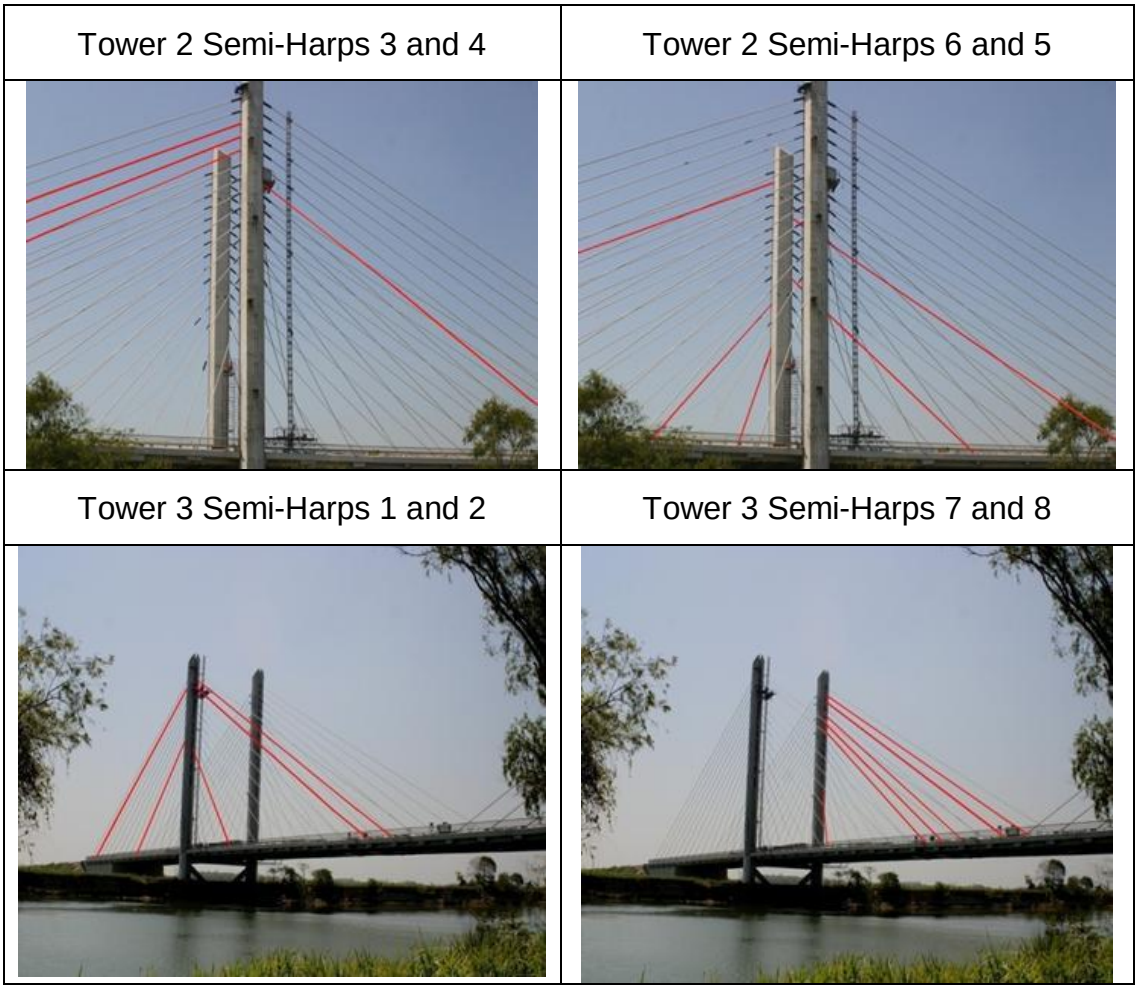

Figure 12 - Elements proposed to replace.

3. EVALUATION OF THE ANCHORAGE ELEMENTS DURING REHABILITATION IN 2008

A summary for the characteristics of each one of the upper anchorage elements of the Río Papaloapan Bridge, removed for rehabilitation and for the probabilistic reliability analysis, is presented in Table 3.

Table 3 - Characteristics of the removed anchorage elements

Id number for anchorage element	Anchorage element type	Semi-Harp	Cable	Deficiency
1	2	1	13	Large grain size
2	2	2	12	Large grain size
3	2	2	13	Large grain size
4	2	3	10	Probable large grain size
5	2	3	11	Large grain size
6	2	3	12	Probable large grain size
7	2	4	8	Probable large grain size
8	2	5	10	Probable large grain size
9	3	6	3	High pore content
10	2	6	13	Large grain size
11	1	7	1	High pore content
12	2	7	8	Large grain size
13	2	7	9	Probable large grain size
14	2	7	10	Large grain size
15	2	7	12	Large grain size
16	2	7	13	Probable large grain size
17	2	1	6	Good condition
18	3	2	4	Good condition
19	2	5	5	Good condition
20	1	6	1	Good condition

The general procedure applied for the rehabilitation of the anchorage elements was the following (Fig.13):

(a) Direct weighting of the cable with a hydraulic jack to measure its tension.
(b) Distension of the cable; each cable was released from its bottom anchorage and then, unscrewed from the upper anchorage element.
(c) Concrete removal to release the upper anchorage up to 5 cm away from the welded union in the tapered plate.
(d) Nondestructive evaluation using penetrant inspection (PT), ultrasonic inspection (UT) and vibration measurements.
(e) Anchorage removal.
(f) Welding of the new anchorage element and rehabilitation of the concrete.
(g) Laboratory inspection of removed elements, including sand blast, PT and UT detailed inspections, and specimens preparation for tension, fracture mechanics and fatigue testing, and microstructural and chemical analyses.

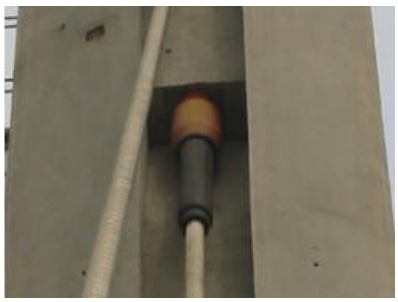

(a) Cable in service

(b) Hydraulic jack for direct weighting

(c) Cable distension

(d) Concrete removal

(e) Non destructive evaluation

(f) Elements in laboratory ready for inspection

Figure 13 - Pictures showing the general process used for the rehabilitation of the upper anchorage elements.

3.1 Vibrations measurements

Cable tension on cable stayed bridges is a key parameter to evaluate the bridge's structural behavior and, in some cases, to elaborate maintenance programs where re-tensioning is necessary to preserve optimal operational conditions. Traditionally, the cable's tension is measured through load tests where an hydraulic jack is fixed to the lower anchorage element of the cable and supported directly by the bridge deck; when the pressure in the jack is increased to the point where the anchorage element is released from the bridge deck, the load supported by the jack is the same to the load carried out by the cable. Although the load tests are highly accurate, the great disadvantages are the time required for setting and for getting off the equipment, the access to the supporting elements, and the temporary traffic disruption for the measurements. As a consequence, the time and cost required for load tests for a bridge with 112 cables, increase significantly. A fast, simple and inexpensive technique to determine indirectly the cable's tension is through the measurement of the vibration frequencies (Fig. 14).

Figure 14 - Typical accelerometer location for the vibration measurements

Cable vibration was measured using a Tec 195 low frequency accelerometer, with a Smart Meter acquisition and processing system, Model 1330 VLF. Accelerometer was fixed to the cable and four independent measurements during a 16 seconds period each, at a sampling rate of 64 Hz were done under normal operation conditions. The number of tests was determined from preliminary test, where acceptable statistical variation was observed considering experimental conditions. Tension of the cable was calculated using a non linear model [10,11].

4. RESULTS FROM INSPECTIONS

4.1 Ultrasonic and liquid penetrant inspection

Ultrasonic and liquid penetrant inspection techniques were used during the rehabilitation process to evaluate the integrity of the upper anchorage elements before removal. Table 4 shows the results from ultrasonic and liquid penetrant inspections in the upper anchorage elements after they were uncovered. In this case, the microstructural evaluation is presented and compared to the previous inspection with embedded elements (Table 3).

Table 4 - Results from ultrasonic (UT) and liquid penetrant (PT) inspections in the anchorage element

Id. No.	Semi-Harp	Cable No.	UT Grain Size Qualification		UT Flaw Detection		PT Crack Detection	
			Embedded elements	Uncovered elements	No. flaws	Total length [mm]	No. cracks	Total length [mm]
1	1	13	Large	Large	----	----	cluster	31.0
2	2	12	Large	Large	----	----	----	----
3	2	13	Large	Large	----	----	----	----
4	3	10	Probable large	Large	----	----	----	----
5	3	11	Large	Large	2	18.5	1	63.0
6	3	12	Probable large	Large	----	----	----	----
7	4	8	Probable large	Large	----	----	1	76.0
8	5	10	Probable large	Large	----	----	----	----
9	6	3	Fine w/pores	Fine w/pores	----	----	----	----
10	6	13	Large	Large	----	----	----	----
11	7	1	Fine w/pores	Fine w/pores	----	----	1	83.0
12	7	8	Large	Fine w/pores	----	----	----	----
13	7	9	Probable large	Large	----	----	----	----
14	7	10	Large	Large	----	----	----	----
15	7	12	Large	Large	----	----	----	----
16	7	13	Probable large	Large	----	----	----	----
17	1	6	Good condition	Fine	----	----	----	----
18	2	4	Good condition	Fine	----	----	----	----
19	5	5	Good condition	Fine	----	----	5	66.0
20	6	1	Good condition	Fine	1	14.0	1	50.0

Fig. 15 shows the pictures of the most critical cracks detected with penetrant testing in the anchorage elements. From this, it can be seen that cracking is not only present in large grain size elements, but also in fine grain size microstructure. It is also important to note that Fig. 15(a) and 15(b) have the same cracking pattern and are present in the heat affected zone (HAZ), while the other two cases, Fig. 15(c) and 15(d), report different behavior with one or several cracks concentrated in one region away from the HAZ.

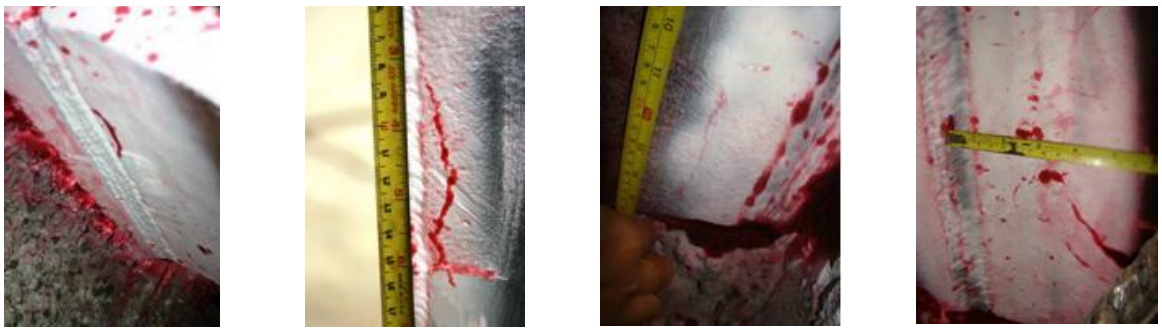

(a) Element Id. No.5 Large grain size | (b) Element Id. No. 7 Large grain size | (c) Element Id. No. 11 Fine grain size w/pores | (d) Element Id. No. 19 Fine grain size

Figure 15 - Cracks detected with liquid penetrant testing (PT) in the anchorage elements

Flaws and cracks detected from the inspections on the welded union are reported in Table 5 and pictures from the penetrant inspections are shown in Fig. 16 (elements not included in table 5 had no flaws or cracks). As it can be seen, flaws were detected with ultrasonic inspection in one case, for an anchorage element with fine grain size but with high pore content. At the same time, with penetrant inspections, critical cracks were identified in three different welds with no clear correlation to the grain size, but most probably to the welding process quality.

Table 5 - Results from ultrasonic (UT) and liquid penetrant (PT) inspections in the welded union

Id. No.	Semi-Harp	Cable No.	UT Flaw Detection		PT Crack Detection	
			No. flaws	Total length [mm]	No. cracks	Total length [mm]
9	6	3	4	7.2	----	----
10	6	13	----	----	3	50
12	7	8	----	----	1	110
17	1	6	----	----	1	50

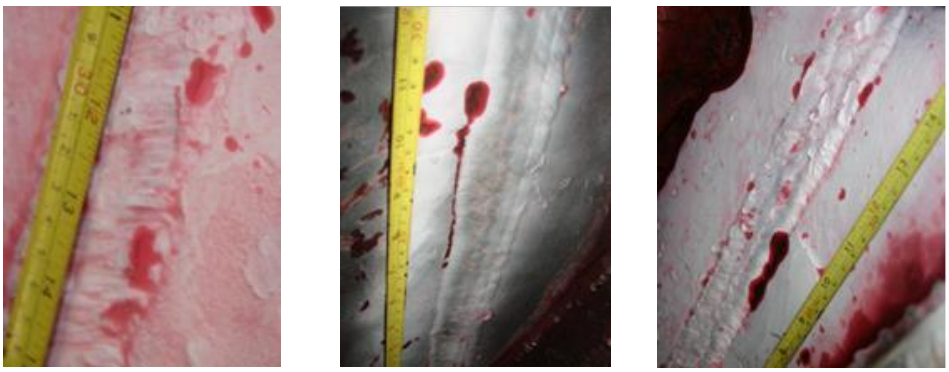

(a) Element Id. No. 10 | (b) Element Id. No. 12 | (c) Element Id. No. 17

Figure 16 - Cracks detected with liquid penetrant testing (PT) in the welded union

4.2 Vibrations measurements

4.2.1 Initial reference and asphalt carpet removal

While the bridge was going into a complete rehabilitation, it was also decided to rehabilitate the bridge surface to meet the geometrical and roughness standards. Taking advantage of this, the supporting material and the asphalt on one side of the bridge deck (two lanes) were removed prior to the distension of the cables on that same side; this to reduce the dead loads of the bridge and to lessen the effect on the remaining cables. As a consequence, the rehabilitation program was first done on semi-harps 1 to 4 on the down stream side; and completed on semi-harps 5 to 7 on the up stream side.

Initial vibration measurements, prior to the rehabilitation, were used for reference. Fig. 17 shows the tensions on the cables in two semi-harps after removal of the asphalt on the down stream side and compared to the reference data. In this figure, it can be seen the difference between two opposite side semi-harps, where the average load decrease per cable in semi-harp 2 (on the down stream side) is 205 N, while for cables in semi-harp 7 (on the up stream side) is 107 N.

Full calculation of the total vertical load reduction in the 112 cables, resulted in 9181 kN. Estimation from the total material removed from the bridge deck was 9326 kN, which represents a 1.55% difference.

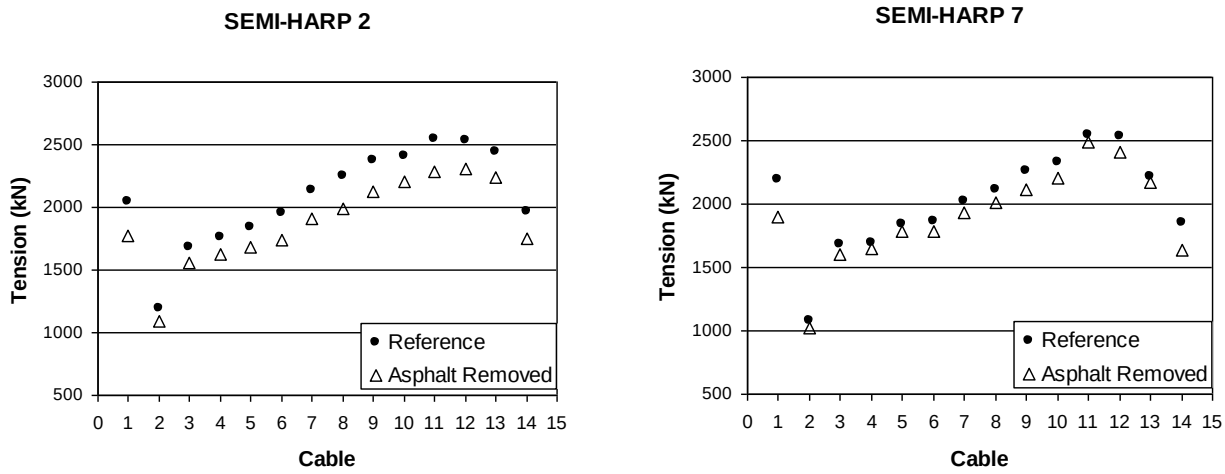

Figure 17 - Tension loads after asphalt removal on cables in semi-harps 2 and 7, with respect to the initial reference tensions.

4.2.2 One cable distension

The first cable to be removed was cable 10 in semi-harp 3. In this case, cables tensions were compared to the asphalt removed data. Figure 18 shows the total load variation along the bridge at each side (down stream and up stream), where the influence of the cable distension affected mainly the 5 neighboring cables. Initial tension in cable 10 was 2363 kN and its corresponding vertical load was 1059 kN. Calculation of the vertical load changes in the 111 remaining cables resulted in 1129 kN, which corresponds to a 6.6% difference. If variations are calculated considering only the 7 closest neighboring cables, the total vertical increase is 1070 kN, which is within 1.1% difference; from this, it is concluded that the total cumulative error from the 112 cables is within 5.5%.

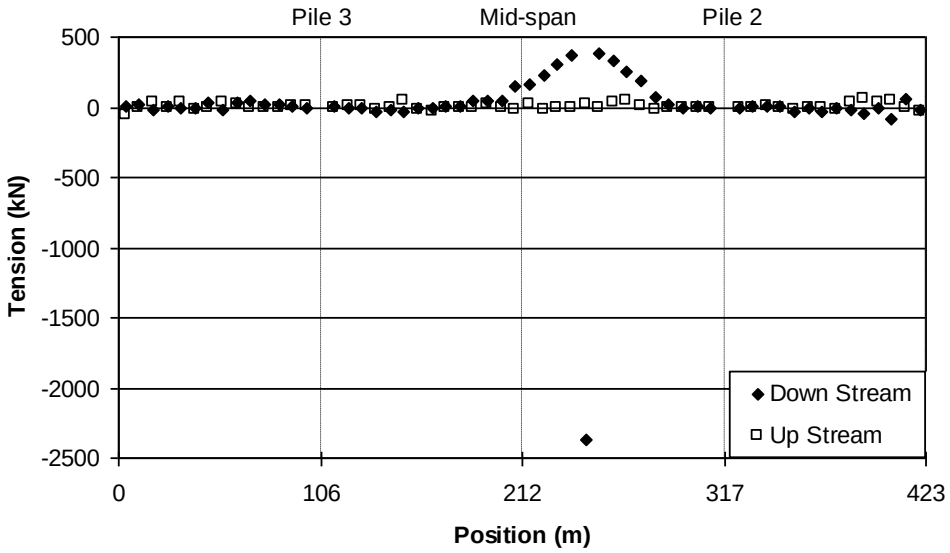

Figure 18 - Variation of the tension on the cables along the bridge after distension of cable 10 in semi-harp 3 (the x axis represents the position of the lower anchorage of each cable).

Figure 19 shows the comparison among the tensions in the cables of semi-harp 3 in the reference condition, after removal of the asphalt on body B, and after the removal of cable 10. From this analysis, the load tensions on the contiguous cables to cable 10, show values within the maximum design limit, which is acceptable to a limited time period required for the rehabilitation of the upper anchorage element.

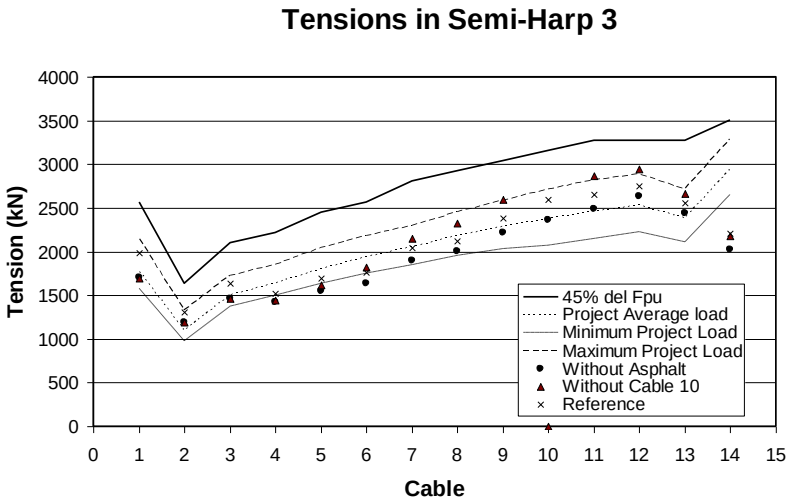

Figure 19 - Monitoring for different load conditions for semi-harp 3 during the first stage of rehabilitation of the bridge.

4.2.3 Two cables distension

To evaluate the condition where two anchorage elements were replaced simultaneously, figure 20 shows the case where cables 6 from semi-harp 1 and 11 from semi-harp 3, were removed. In this case, again it is noted that the distension effect is limited up to the 5 closest neighbors from the removed cable. In this case, the total removed vertical load was 1900 kN, while the total vertical load increase for the 110 remaining cables was 1962 kN; which corresponds to a 3.2% difference. Again, if variation is calculated only to the 7 closest cables, the difference is reduced to 1.4% from the total removed vertical load.

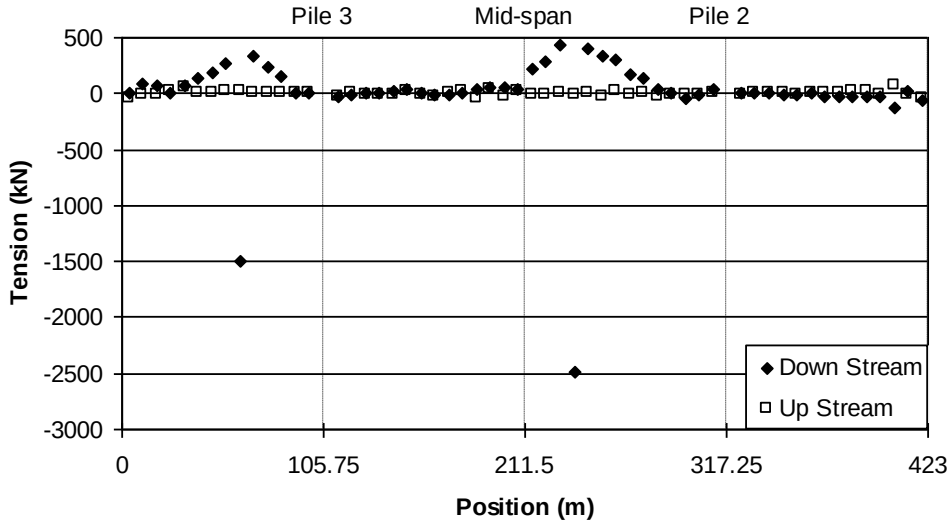

Figure 20 - Variation of the tension on the cables along the bridge after distension of cables 6 in semi-harp 1 and 11 in semi-harp (the x axis represents the position of the lower anchorage of each cable).

4.2.4 Statistical influence of the distension of a cable

Different load conditions were evaluated and statistical vertical load redistribution was calculated for each removed cable condition (Fig. 12). From this analysis, it is shown that the distension of one cable has limited influence to a few neighboring cables; thus bridge behavior can be estimated beforehand (Fig. 21).

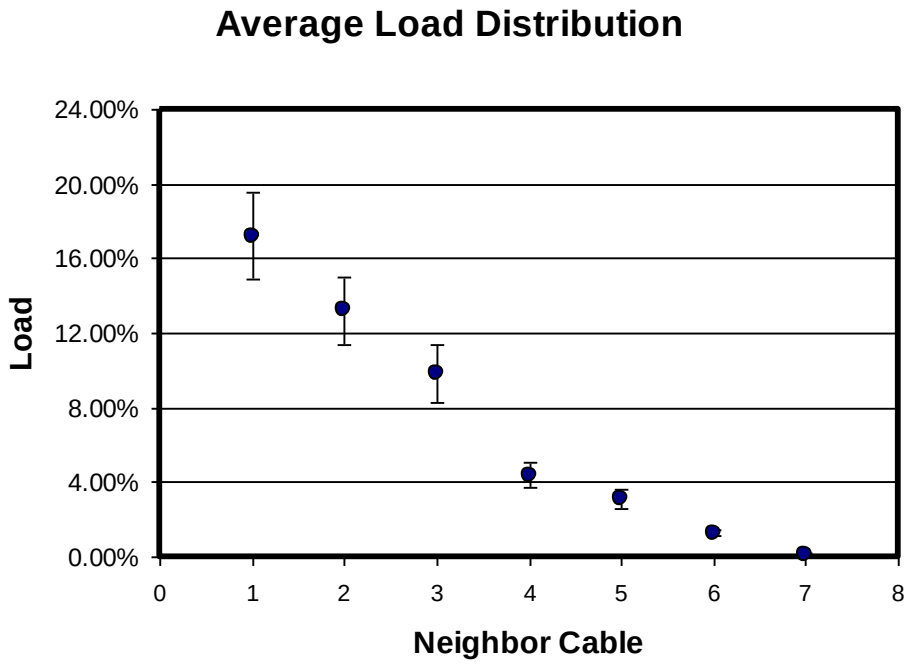

Figure 21 - Average load distribution to neighboring cables for a released cable.

5. CONCLUSIONS

In general, from these results and for this particular case, it was found that ultrasonic inspections for grain size evaluation on the embedded elements, were quite reliable within an accuracy of 95%, that is, 19 elements out of 20 were accurately identified. The element that was initially classified as large grain size and resulted with a fine grain size with a large number of pores, was incorrectly classified because of the pore content, where ultrasonic energy dissipation presents almost the same behavior. At any rate, this anchorage element would be classified as structurally deficient.

From the inspections on the uncovered elements, flaws were identified with ultrasonic testing in the core material in two upper anchorage elements, and from the liquid penetrant testing; cracks were also detected in these two elements. At the same time, in other four elements, cracks were found near the welding area or the heat affected zone (HAZ) using the liquid penetrant technique. Four large cracks in different elements (2 with large grain size and 2 with fine grain size) were detected from direct liquid penetrant and ultrasonic inspections on the welding joints of the anchorage elements to the tapered plate. One of these cracks is internal and it was detected with ultrasonic inspection, while the other three were superficial and detected with liquid penetrant inspection. In general, there is some relation between the microstructural characteristics (grain size, pores and inclusions) and the cracks; but the most significant factor is given by welding and post heat treatment processes.

Statistically speaking, initial ultrasonic inspection on the embedded anchorage elements had a 95% accuracy in the grain size identification, 66% accuracy on recognition of high pore content (2 elements out of three), and 75% accuracy for internal flaw detection.

As initially planned, the main purpose of the ultrasonic inspection on the embedded elements was to identify large microstructural grain size in the steel of the upper anchorage elements, which is fulfilled with a very good accuracy. Detection on internal pores was good enough, since only one element with very high pore content was incorrectly classified as a large grain size element. Internal and superficial flaws and cracks detection were always limited to the sensitivity of ultrasonic inspection and to the limited inspection surface that opened a small window to the interior of the material as previously discussed.

Structural behavior of the Río Papaloapan cable stayed bridge was fully monitored during rehabilitation and it was possible through the measurement of the cables vibration and analysis using a non linear model. Results are within a 2% error if engineering criterion is used to calculate the total loads distributions and to avoid cumulative errors; nonetheless, if all data is included, errors are within 7%.

In general, the complete rehabilitation of the Río Papaloapan Bridge was fully monitored and its structural behavior was secured, even if two cables were replaced simultaneously. Load distributions from the removed cable to the immediate neighbors were in average 17.2%; and the load redistribution affected only to the seventh closest cables.

REFERENCES

1. Carrión, F., Lomelí, G., López, A., Pérez, J., Terán J., and Jiménez R. (2003). Estudio para la Evaluación de los Dispositivos de Soporte Superior (Botellas) de los Anclajes de los Tirantes del Puente Río Papaloapan. Instituto Mexicano del Transporte. Internal Final Report EE05/03. Sanfandila. Qro,. Mexico
2. Astiz, M. A. (1997). Composite construction in Cable-Stayed Bridge Towers. International Conference on Composite Construction - Conventional and Innovative. Conference Report. 16-18 September. Innsbruck. Austria. pp 127-132
3. Aguirre A., and Carbajal J. (2000). Análisis de Falla en el Tirante no. 11 del Puente Papaloapan. Corporación Mexicana de Investigación en Materiales SA de CV. Internal Report **AF-IFT/00-087.** Saltillo. Coah,. Mexico
4. López A., and Poblano C. (2000). Análisis de Falla y Pruebas de Fatiga del Anclaje Desprendido del Tirante 11, Lado Agua, Torre 3, del puente Río Papaloapan. Instituto Mexicano del Transporte. Internal Final Report **EQ001/00**. Sanfandila, Qro,. Mexico
5. ASTM. (1998). Standard Specification for Steel Castings, High Strength, for Structural Purposes. ASTM Designation **A148/A 148M-93B (Rev.98)**. West Conshohocken. PA. USA
6. Anderson T. L. (1991). Fracture Mechanics - Fundamentals and Applications. CRC Press. Boca Raton. USA
7. ASTM. (2005). Standard Test Method for Linear-Elastic Plane-Strain Fracture Toughness K_{IC} of Metallic Materials. ASTM Designation **E399-05**. West Conshohocken. PA. USA
8. ASTM. (2005). Standard Test Method for Measurement of fatigue Crack Growth Rates. ASTM Designation **E 647-05**. West Conshohocken. PA. USA
9. ASM Handbook Committee. (1997). Nondestructive Evaluation and Quality Control. ASM INTERNATIONAL. ASM Handbook. Vol. **17**
10. Carrión-Viramontes F. J., López-López J. A., Quintana-Rodríguez J. A. and Lozano-Guzmán A. (2008) Nonlinear assessment of cable vibration in a stayed bridge. Experimental Mechanics. 48. pp 153-161
11. Carrión Francisco J., López José A., Quintana Juan A. and Orozco Pablo R. (2009). Structural monitoring of a cable stayed bridge Turing rehabilitation. 4th International conference on structural health monitoring on intelligent infrastructure (SHMII-4). Zurich. Switzerland. paper **337**